Computer Networks 100 (2016) 157–165

Contents lists available at ScienceDirect

Computer Networks

journal homepage: www.elsevier.com/locate/comnet

Optimal power distribution in non-binary LDPC code-based cooperative wireless networks

Bruna L.R. Melo[a], Daniel C. Cunha[b,*], Cecilio Pimentel[c]

[a] Third Center for Integrated Air Defense and Air Traffic Control (CINDACTA III), Av. Centenário Alberto Santos Dumont, Recife, PE s/n - 51250-000, Brazil

[b] Centro de Informática (CIn), Federal University of Pernambuco (UFPE), Av. Jornalista Anibal Fernandes, Recife, PE s/n - 50740-560, Brazil

[c] Department of Electronics and Systems (DES), Federal University of Pernambuco (UFPE), Av. da Arquitetura, Recife, PE s/n - 50740-550, Brazil

ARTICLE INFO

Article history:
Received 20 April 2015
Revised 9 October 2015
Accepted 19 February 2016
Available online 5 March 2016

Keywords:
Channel capacity
Cooperative communications
Flat fading channels
Non-binary LDPC codes
Outage probability
Power optimization

ABSTRACT

This work analyzes the optimal power allocation in coded cooperative communication systems with a single relay and using the amplify-and-forward protocol. Non-binary low-density parity-check (LDPC) codes are used at the source and a fast Fourier transform (FFT)-based decoding algorithm is employed at the destination. We study the power distribution between the source and the relay based on the minimization of the LDPC bit error rate (BER) performance at the destination as well as on the information theoretic measures such as the channel capacity and outage probabilities. The optimal power allocation estimated by the LDPC performance simulation corresponds to the capacity/outage probability results. In addition, BER comparisons of the coded systems (cooperative and noncooperative) are carried out for some typical cooperative scenarios.

1. Introduction

Internet of Things is an emerging paradigm where various objects (or things) are able to connect to the Internet using technologies as wireless sensor networks [1], radio frequency identification [2], Wi-Fi [3] and cellular networks [4]. In a wireless sensor network, many sensor nodes are used to monitor physical or environmental conditions and utilize wireless communications to transmit information to each other [5]. An efficient strategy to cope with the impairments offered by the wireless communication channel is to employ a cooperative protocol between spatially distributed nodes. Several protocols, including amplify-and-forward (AF), decode-and-forward (DF), estimate-and-forward (EF) are widely used [6]. Since the sensor nodes have limited energy supply, energy efficiency is a crucial issue in the design of cooperative communication protocols.

Optimal power allocation is an important question in performance enhancement of cooperative network protocols. In [7], the optimal power allocation and the associated symbol error rate performance were studied for AF and DF protocols under different modulation schemes. A similar investigation was done in [6] where the performance analysis and optimal power allocation for the EF protocol depend on the modulation scheme. Recently, optimal power allocation and adaptive modulation were used in AF cooperative protocols [8], where the objective was to find the signal-to-noise ratio (SNR) regions for adaptive modulation schemes considering a bit error rate (BER) constraint.

Binary low-density parity-check (LDPC) coding strategies have been used to improve the performance of cooperative communication protocols [9,10]. To perform close

* Corresponding author. Tel.: +558121268430.
E-mail addresses: brunalaisrochamelo@gmail.com (B.L.R. Melo), dcunha@cin.ufpe.br (D.C. Cunha), cecilio@ufpe.br (C. Pimentel).

http://dx.doi.org/10.1016/j.comnet.2016.02.022
1389-1286/

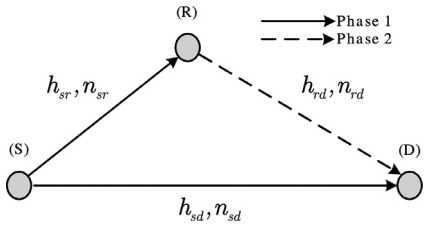

Fig. 1. Model of the cooperative communication system using a single relay.

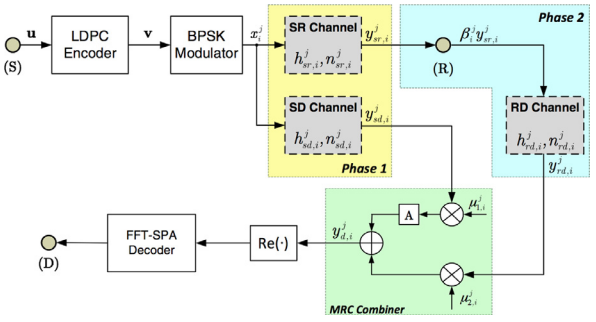

Fig. 2. Block diagram of the coded cooperative communication system from the modulator output to the MRC combiner output (the diagram highlights the binary components of the signals). (S), (R), and (D) represent, respectively, source, relay, and destination, while $Re(\cdot)$ indicates the real part of the signal $y^j_{d,i}$.

to the theoretical limit, binary LDPC codes require large blocklengths, leading to high transmission latency and complex decoding. Since it is not desirable in the real world communications, we consider the investigation of non-binary LDPC codes, motivated by their strong decoding performance for short-to-moderate blocklengths [11]. Short-to-moderate LDPC codes have been applied to enhance the performance of practical wireless communications systems [12].

Works at physical layer are significant to get efficient power allocation strategies, not only considering modulation but also including error control coding schemes. In this work, we present an analysis of the optimal power allocation in an AF coded cooperative network with a single relay. We consider both short-length binary and non-binary LDPC codes. The BER of the coded AF protocol as well as information theoretical measures (channel capacity and outage probability) are used as performance metrics to find the optimal power distribution between the source and the relay in two cooperative scenarios. These metrics are obtained from the conditional formula for the maximum average mutual information of the AF protocol. Then, we resort to a semi-analytical approach that simulates the fading effect through Monte Carlo integration. We compare the performance of optimal power allocation scheme with that of equal power allocation one. We also compare the power allocation and the system performance of the cooperative system to those of the point-to-point communication system.

The outline of the paper is as follows. In Section 2, we present the description of the cooperative system model and the decoding algorithm used at the destination. Numerical BER and channel capacity results of the optimal power allocation for fast fading are shown in Sections 3 and 4, respectively, while the outage probability is employed in Section 5 to study the optimal power allocation in block fading channels. Finally, conclusions are drawn in Section 6.

2. System description

2.1. Cooperative system model

Consider the cooperative communication system illustrated in Fig. 1, where a source (S) sends information directly and through a relay (R) to a destination (D) [6]. Assume that source and relay transmit their data through orthogonal channels and that time division multiple access (TDMA) is done. Solid lines in Fig. 1 represent the broadcast performed by the source in the first time slot (phase 1), while the dot line represents the routing from the relay to the destination in the second interval.

Fig. 2 shows a block diagram of the cooperative communication system adopted in this work. In the first stage, the source encodes a vector of k information symbols $\mathbf{u} = [u_1, \ldots, u_k]$ using a non-binary LDPC code $C(n, k)$ defined in $GF(q), q = 2^m$ and m a positive integer, in a vector of n coded symbols $\mathbf{v} = [v_1, \ldots, v_n]$. After that, the source transmits (broadcasts) the q-ary codeword $\mathbf{v}$ to the relay and the destination. For each coded symbol v_i, its corresponding binary vector of m bits $\mathbf{c}_i = [c_i^1, \ldots, c_i^j, \ldots, c_i^m]$ is mapped into an vector of antipodal signals $\mathbf{x}_i = [x_i^1, \ldots, x_i^j, \ldots, x_i^m]$ ($x_i^j \in \{-1, +1\}$) and sent through source-relay (SR) and source-destination (SD) channels. For the jth bit of the ith transmitted symbol, the received signals at the relay and at the destination, denoted by $y^j_{sr,i}$ and $y^j_{sd,i}$, are given by

$$y^j_{sr,i} = \sqrt{E_s} h^j_{sr,i} x^j_i + n^j_{sr,i} \tag{1}$$

and

$$y^j_{sd,i} = \sqrt{E_s} h^j_{sd,i} x^j_i + n^j_{sd,i}\,, \tag{2}$$

where E_s is the energy of the transmitted signal from the source, and $n^j_{sr,i}$ and $n^j_{sd,i}$ represent additive white Gaussian noise (AWGN). In (1) and (2), $h^j_{sr,i}$ and $h^j_{sd,i}$ represent multiplicative gains due to the flat fading of the SR and SD channels, respectively. Both gains are modeled by independent zero-mean complex Gaussian random variables with variances σ^2_{sr} and σ^2_{sd}, respectively. In addition, we assume that $h^j_{sr,i}$ and $h^j_{sd,i}$ vary independently bit to bit (recall that we are using a binary modulation) and that they are known at the receiver. Without loss of generality, we consider that $n^j_{sr,i}$ and $n^j_{sd,i}$ are modeled as zero-mean complex Gaussian random variables with variance N_0.

In the second stage, the relay only amplifies the received analog signal $y^j_{sr,i}$ and forwards it to the destination.

The received signal at D (sent by R) is then given by

$$y^j_{rd,i} = \beta^j_i h^j_{rd,i} y^j_{sr,i} + n^j_{rd,i} \tag{3}$$

where $h^j_{rd,i}$ is the gain of the relay-destination (RD) channel, modeled as a zero-mean complex Gaussian random variable with variance σ^2_{rd}. The noisy term $n^j_{rd,i}$ is also modeled as a zero-mean complex Gaussian random variable with variance N_0 and β^j_i is the amplification factor that characterizes the AF protocol.

Similar to $h^j_{sr,i}$ and $h^j_{sd,i}$, $h^j_{rd,i}$ is known at the receiver and varies independently bit to bit. This corresponds to the fast fading environment. For this reason, the cooperative protocol assumed in this section is named variable gain AF protocol, whose amplification factor β^j_i is [6]

$$\beta^j_i = \sqrt{\frac{E_r}{E_s|h^j_{sr,i}|^2 + N_0}} \tag{4}$$

where E_r is the energy of the transmitted signal from the relay. The factor β^j_i is applied such that the energy of the signal $\beta^j_i y^j_{sr,i}$ becomes equal to the energy of the signal sent from relay, that is, $E\left[|\beta^j_i y^j_{sr,i}|^2\right] = E_r$ [6], being $E[\,\cdot\,]$ the expectation operator. Substituting (1) and (4) into (3), we find the equivalent model of the source-relay-destination (SRD) channel as

$$y^j_{rd,i} = (h^j_{rd,i})' x^j_i + (n^j_{rd,i})' \tag{5}$$

where $(h^j_{rd,i})'$ is the equivalent multiplicative gain [6]

$$(h^j_{rd,i})' = \sqrt{\frac{E_s E_r}{E_s|h^j_{sr,i}|^2 + N_0}} h^j_{rd,i} h^j_{sr,i} \tag{6}$$

and $(n^j_{rd,i})'$ is the equivalent additive noise [6]

$$(n^j_{rd,i})' = \sqrt{\frac{E_r}{E_s|h^j_{sr,i}|^2 + N_0}} h^j_{rd,i} n^j_{sr,i} + n^j_{rd,i}\,. \tag{7}$$

Since $n^j_{sr,i}$ and $n^j_{rd,i}$ are independent random variables, the equivalent noise $(n^j_{rd,i})'$ is modeled as a zero-mean complex Gaussian random variable with variance ρ^2_e given by [6]

$$\rho^2_e = \left(\frac{E_r|h^j_{rd,i}|^2}{E_s|h^j_{sr,i}|^2 + N_0} + 1\right) N_0\,. \tag{8}$$

The received signals at the destination at the end of each stage, $y^j_{sd,i}$ and $y^j_{rd,i}$, given by (2) and (5), respectively, are added by a maximum-ratio combiner (MRC)[13]. The block "A" illustrated in Fig. 2 represents a delay block, since the MRC needs to wait for two transmissions. Then, the output of the MRC is expressed by $y^j_{d,i} = \mu^j_{1,i} y^j_{sd,i} + \mu^j_{2,i} y^j_{rd,i}$, where $\mu^j_{1,i}$ and $\mu^j_{2,i}$ are given by [6]

$$\mu^j_{1,i} = \frac{\sqrt{E_s}(h^j_{sd,i})^*}{N_0} \tag{9}$$

and

$$\mu^j_{2,i} = \frac{\sqrt{\dfrac{E_r E_s}{E_s|h^j_{sr,i}|^2 + N_0}}(h^j_{rd,i})^*(h^j_{sr,i})^*}{\rho^2_e} \tag{10}$$

where $(h^j_{wz,i})^*$ represents the complex conjugate of the multiplicative gain of the wz channel, with $w \in \{s, r\}$ and $z \in \{r, d\}$. Finalizing the MRC process, the real part of the output signal $y^j_{d,i}$ (block identified by "$Re(\,\cdot\,)$" in Fig. 2) is extracted and passed to the decoder.

2.2. FFT-based decoding algorithm

The sum-product (SP) algorithm proposed in [11] for decoding non-binary LDPC codes has computational complexity of order $O(q^2)$ due to the multiplications performed in the calculation of check nodes messages. MacKay and Davey introduced the FFT in the calculation of the check nodes messages, reducing the decoding complexity to $O(q\log_2 q)$ [14]. Therefore, a new iterative decoding algorithm was proposed in [15] and is denoted in this work by FFT-SP algorithm.

The FFT-SP algorithm operates based on the exchange of messages (that represent *a priori* probabilities of the coded symbols) in a factor graph [16]. In the context of error correcting codes, factor graphs are graphical representations which have two types of nodes: variable nodes, corresponding to the n symbols of the transmitted codeword $\mathbf{v}$ and check nodes, which correspond to the $(n-k)$ parity check equations of the code. The connections between the variable nodes and check nodes allow the exchange of messages (iteratively) resulting, by some stopping criterion, in obtaining the estimate of the transmitted codeword. A summary of the FFT-SP algorithm is described in Appendix A [17].

3. Optimal power allocation for LDPC coded cooperative system

Computer simulations are performed for the LDPC coded cooperative and noncooperative systems considering the channel model described in Section 2.1 (fast fading). To simplify the nomenclature, the noncooperative systems are denominated *direct link* (DL) systems. We assume in both systems the binary regular LDPC code $C_1(1000, 500)$ and the 4-ary LDPC code $C_2(500, 250)$ in such way that both codes have the same codeword length (in bits). The AWGN variance is assumed unitary (i.e., $N_0 = 1$) and the gain variance of the SD channel is normalized to 1 (i.e., $\sigma^2_{sd} = 1$). We consider two cooperative scenarios, depending on the relative quality of the SR and RD channels. In the first cooperative scenario, the quality of the SR and RD channels are similar, that is, $\sigma^2_{sr} = \sigma^2_{rd} = 1$; this scenario can be interpreted as the relay in the middle of the distance between the source and the destination. In the second scenario, the SR channel is better than the RD channel (we assume $\sigma^2_{sr} = 10, \sigma^2_{rd} = 1$); in this case, the relay is closer to the source than the destination. For the cooperative systems, the total transmission energy E_t is divided between

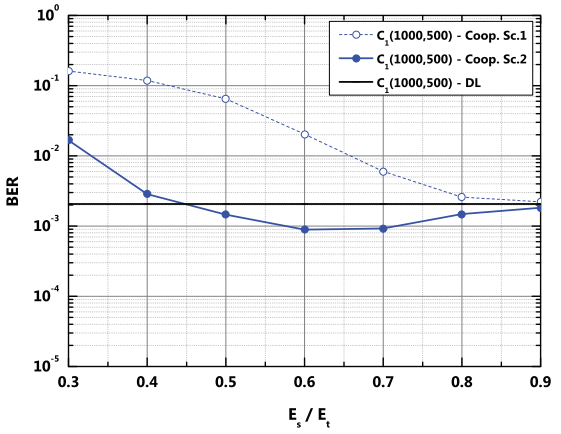

Fig. 3. BER versus the energy ratio E_s/E_t for the binary LDPC code $C_1(1000, 500)$ considering the two cooperative scenarios and the direct link. The total signal-to-noise ratio, E_t/N_0, is 4.5 dB.

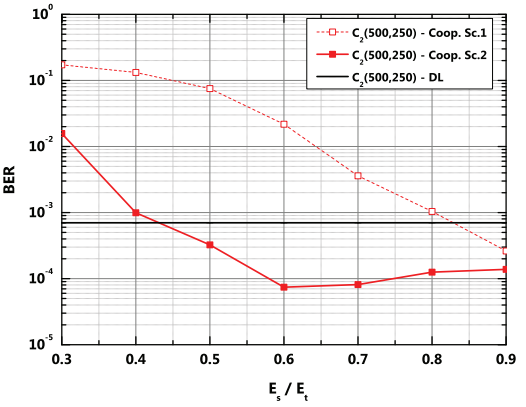

Fig. 4. BER versus the energy ratio E_s/E_t for the 4-ary LDPC code $C_2(500, 250)$ considering the two cooperative scenarios and the direct link. The total signal-to-noise ratio, E_t/N_0, is 4.5 dB.

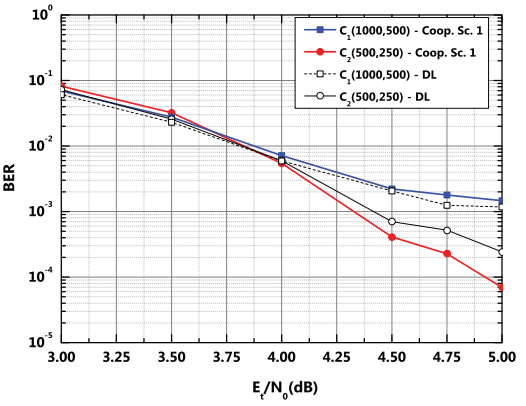

Fig. 5. BER versus the signal-to-noise ratio E_t/N_0 (in dB) for the first cooperative scenario and the direct link (DL). In each case, the binary LDPC $C_1(1000, 500)$ and the 4-ary LDPC code $C_2(500, 250)$ are used for an optimized energy ratio $E_s/E_t = 0.9$.

the source transmitted energy E_s and the relay transmitted energy E_r, i.e., $E_t = E_s + E_r$, for a fair comparison with the DL systems. At last, in both cases (cooperative and DL), the decoding algorithm used in the destination is the FFT-SP algorithm described in Appendix A with 50 iterations.

The energy ratio E_s/E_t represents the power distribution between the source and the relay in a single-relay cooperative communication system. We investigate in this section the optimal ratio E_s/E_t that achieves the best performance of binary and non-binary LDPC coded systems operating in two cooperative scenarios under the fast fading environment.

Fig. 3 shows the BER versus the energy ratio E_s/E_t for the binary LDPC code $C_1(1000, 500)$ considering the two cooperative scenarios for $E_t/N_0 = 4.5$ dB. The performance of the DL system is also illustrated in Fig. 3. As expected, the performance of the DL system is constant (equal to $2 \cdot 10^{-3}$), since this configuration is a point-to-point communication, i.e., there is no presence of the relay. For the first cooperative scenario ($\sigma_{sr}^2 = \sigma_{rd}^2 = 1$), we observe that the system performance only becomes similar to the DL performance when $E_s/E_t = 0.9$. In other words, the cooperative system only has an equivalent performance to the DL one, if the source have 90% of the total transmitted energy. As the SR and SD channels have the same quality (which is measured by the channel gain), we see that it is better to transmit the information directly to the destination. In the second scenario, it is more advantageous to employ cooperative communications when the source has at least 45% of the total energy E_t. Considering the use of the LDPC code $C_1(1000, 500)$, the optimal energy ratios E_s/E_t are 0.9 and 0.6 for the first and the second cooperative scenarios, respectively.

The same analysis is performed for the 4-ary LDPC code $C_2(500, 250)$ and it is illustrated in Fig. 4. The performance of the DL 4-ary coded system is equal to $7 \cdot 10^{-4}$ for all range of the energy ratio E_s/E_t. This value is used as a reference as in the binary case. Considering the first cooperative scenario, we can see that the performance of the 4-ary coded cooperative system becomes better than the reference from $E_s/E_t = 0.83$ approximately (this improvement in performance cannot be observed in the first scenario in Fig. 3 for the binary LDPC code). When the relay is close to the source (which means that the SR channel has better average SNR than the SD channel), the performance of the 4-ary coded cooperative system improves from $E_s/E_t = 0.43$. In a similar manner to the binary LDPC code C_1, the optimal energy ratios are 0.9 and 0.6 for the first and the second cooperative scenarios, respectively, when the 4-ary LDPC code C_2 is used. This is also valid for other codeword lengths (curves not shown). The benefit of using the optimal energy ratio is more pronounced for non-binary codes, because the performance degrades significantly as E_s/E_t changes from the optimal values.

The BER performance versus the signal-to-noise ratio E_t/N_0 for both codes C_1 and C_2 as well as the DL is compared in Fig. 5 for the first cooperative scheme with the optimized energy ratio. While the cooperative system with the binary code has no important advantage over the DL, the performance gain achieved by the non-binary code over the corresponding DL increases as E_t/N_0 increases. A similar conclusion is drawn from Fig. 6 where the second

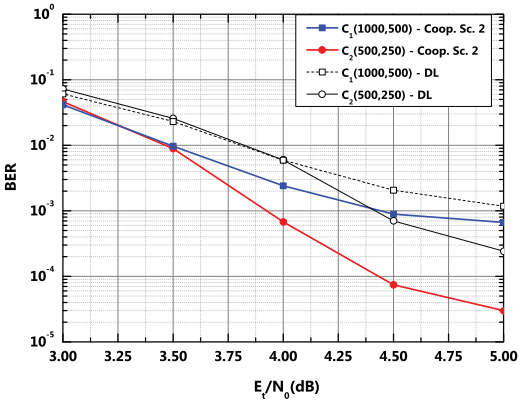

Fig. 6. BER versus the signal-to-noise ratio E_t/N_0 (in dB) for the second cooperative scenario and the direct link (DL). In each case, the binary LDPC $C_1(1000, 500)$ and the 4-ary LDPC code $C_2(500, 250)$ are used for an optimized energy ratio $E_s/E_t = 0.6$.

scenario is considered with the corresponding optimal energy ratio.

4. A channel capacity study

In this section, we numerically study the optimal energy ratio of the AF protocol described in Section 2.1 (fast fading) from an information-theoretic perspective. As observed in Section 2.1, the AF protocol at the output of the MRC can be viewed as an equivalent fading channel with a single input and a single output. For fixed fading realizations, the maximum average mutual information is achieved by independent and identically distributed circularly symmetric complex Gaussian inputs and is given by [18]

$$I_{AF}(h^j_{sd,i}; h^j_{sr,i}; h^j_{rd,i}) = \frac{1}{2}\log_2\left(1 + E_s/N_0|h^j_{sd,i}|^2 + \frac{E_s/N_0|h^j_{sr,i}|^2 \cdot E_r/N_0|h^j_{rd,i}|^2}{E_s/N_0|h^j_{sr,i}|^2 + E_r/N_0|h^j_{rd,i}|^2 + 1}\right). \quad (11)$$

Then, $I_{AF}(h^j_{sd,i}; h^j_{sr,i}; h^j_{rd,i})$ is a random variable with probability density function determined by the channel fading gains. The channel capacity C is expressed as

$$C = E[I_{AF}(h^j_{sd,i}; h^j_{sr,i}; h^j_{rd,i})]$$

where the expected value is taken with respect to the fading gains. We provide in the following the numerical channel capacity evaluation obtained from Monte Carlo integration. In Fig. 7, we display the channel capacity versus the energy ratio E_s/E_t, for $E_t/N_0 = 4.5$ dB, for the two cooperative scenarios considered in this work. The optimal energy ratio indicated by the maximization of the capacity curves is in generally good agreement with the BER analysis of the LDPC codes conducted in the previous section. We repeat this analysis for a broad range of E_t/N_0 and present the optimal energy ratio versus E_t/N_0 in Fig. 8. For low values of

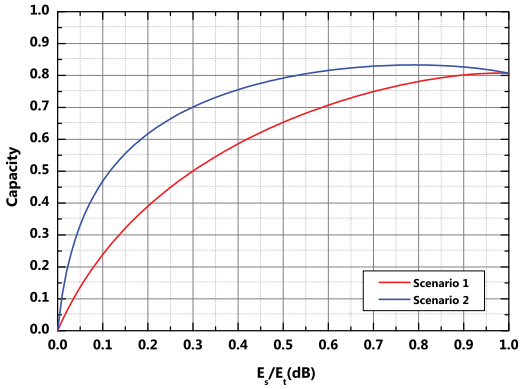

Fig. 7. Channel capacity versus the energy ratio E_s/E_t considering the two cooperative scenarios for $E_t/N_0 = 4.5$ dB.

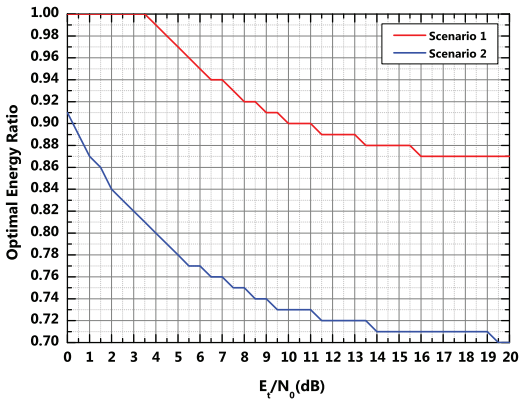

Fig. 8. Optimal energy ratio E_s/E_t versus the total signal to noise ratio E_t/N_0 (in dB) considering the two cooperative scenarios.

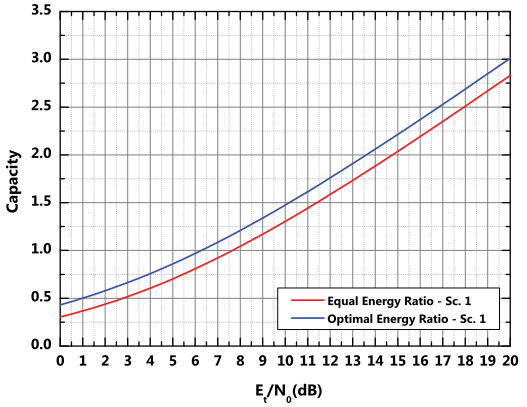

Fig. 9. Channel capacity comparison for the equal energy ratio and the optimal energy ratio considering the first cooperative scenario.

E_t/N_0, the capacity curve for the second scenario provides a steeper slope and the optimal energy ratios E_s/E_t tend to approximately 0.9 and 0.7 for the first and the second scenarios, respectively, in the regime of high E_t/N_0.

Figs. 9 and 10 compare the channel capacity of the optimal energy ratio scheme with that of the equal energy ratio. The capacity gain provided by the optimal energy ratio

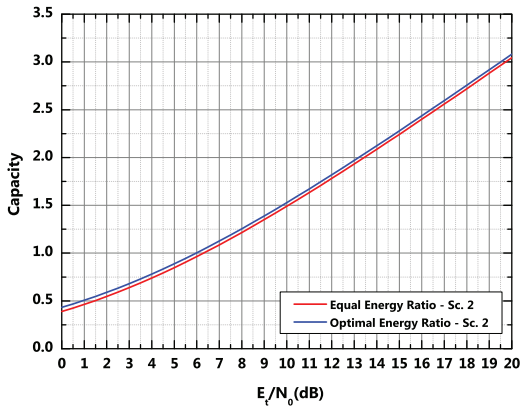

Fig. 10. Channel capacity comparison for the equal energy ratio and the optimal energy ratio considering the second cooperative scenario.

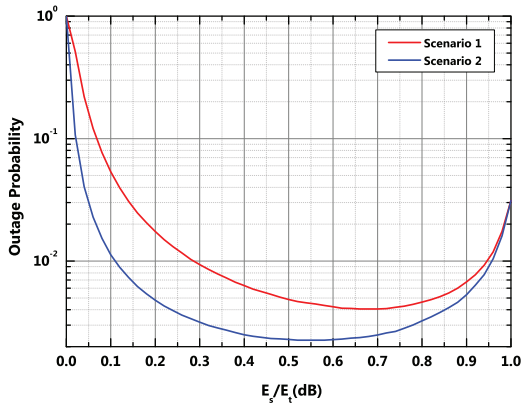

Fig. 11. Outage probability versus the energy ratio E_s/E_t considering the two cooperative scenarios for $E_t/N_0 = 15$ dB.

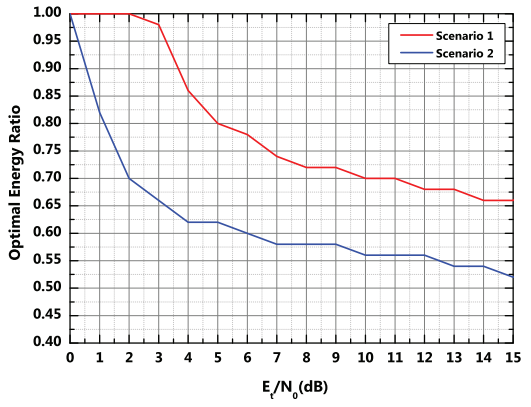

Fig. 12. Optimal energy ratio E_s/E_t versus the total signal to noise ratio E_t/N_0 (in dB) considering the two cooperative scenarios.

in the second scenario is negligible and the equal power allocation tends to be the optimal scheme when the relay gets closer to the source.

5. Optimal energy ratio for block fading channel

In this section, we study the optimal energy ratio for the AF protocol for quasi-static block-fading environments. We assume that the fading gains $h_{sr,\,i}$, $h_{sd,\,i}$ and $h_{rd,\,i}$ remain constant during the transmission of the ith codeword and changes independently from one codeword to the next. In this model, a deep fade affects many consecutive bits within a codeword leading to large number of bit errors. The primary measure of interest for this system model is the outage probability [19]. This probability is defined for infinite blocklength code, however, it has shown to predict well the frame error rate (FER) of good finite length codes [20].

The outage probability $P_{\text{out}}(E_s/N_0, E_r/N_0, R)$ is defined as the probability that the information rate R exceeds the mutual information of the channel, thus

$$P_{\text{out}}(E_s/N_0, E_r/N_0, R) = \Pr(I_{AF}(h_{sd,i}; h_{sr,i}; h_{rd,i}) < R) \qquad (12)$$

where the mutual information $I_{AF}(h_{sd,\,i}; h_{sr,\,i}; h_{rd,\,i})$ is provided in (11). Since the analytical evaluation of (12) becomes intractable, we resort to Monte Carlo integration to numerically evaluate the outage probability.

For a fixed E_t/N_0, the optimal energy ratio is determined by the minimization of the outage probability, as is illustrated in Fig. 11, for $E_t/N_0 = 15$ dB. Fig. 12 displays the variation of the optimal energy ratio versus E_t/N_0 for each cooperative scenario.

The FER performance versus the signal-to-noise ratio E_t/N_0 using the optimal energy ratio for both codes C_1 and C_2 is compared in Figs. 13 and 14 for the first and second scenarios, respectively. The outage probability is also shown for comparison. The outage probability curves predict the FER ones very closely with constant gap and slope. It should be remarked that the outage probabilities were calculated with the assumption of Gaussian channel inputs, while BPSK signals are assumed in the simulations of LDPC codes. Fig. 14 reveals that, for block fading channel in the second scenario, the 4-ary code can achieve about 1 dB code gain over the binary code, while the coding gain provided in the first scenario is negligible (see Fig. 13). Thus, the choice of more powerful non-binary codes is effective in increasing the system reliability when the relay is close to the source. We can also see that the order diversity (negative of the slope of the outage probability when plotted in a log-log scale versus E_t/N_0) of two is achieved.

6. Final comments

In this work, we presented an analysis of the optimal power allocation in an LDPC coded cooperative network with a single relay operating with the AF protocol. The BER, channel capacity and outage probability were used as performance metrics to find the optimal power distribution between the source and the relay in two cooperative scenarios. We identify scenarios for which the choice of LDPC codes with non-binary fields provide coding gains relative to LDPC binary codes. In general, the optimal power allocation predicted by the LDPC performance simulation and by the capacity/outage probability results are in good agreement. The equal power allocation scheme tends to the

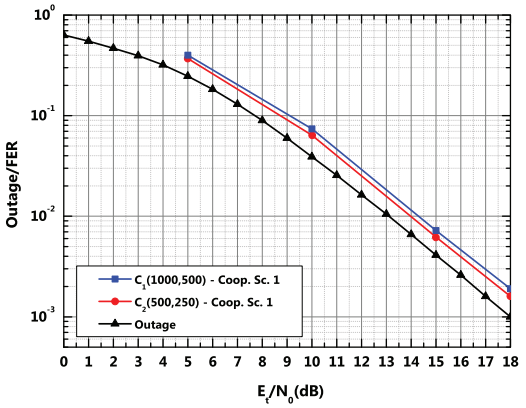

Fig. 13. Comparison between the outage probability and the simulated FER for the first cooperative scenario. In each case, the binary LDPC $C_1(1000, 500)$ and the 4-ary LDPC code $C_2(500, 250)$ are used for an optimized energy ratio.

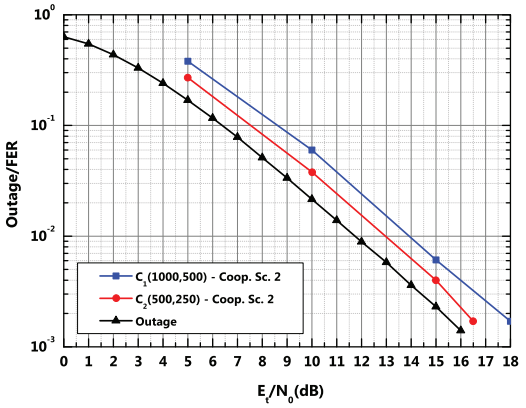

Fig. 14. Comparison between the outage probability and the simulated FER for the second cooperative scenario. In each case, the binary LDPC $C_1(1000, 500)$ and the 4-ary LDPC code $C_2(500, 250)$ are used for an optimized energy ratio.

optimal when the relay gets closer to the source. We compared the power allocation and the system performance of the cooperative system to those of the point-to-point communication system. We also observed that the optimal energy ratio does not depend on the field size.

Acknowledgments

The authors gratefully acknowledge Prof. Richard Demo Souza for his support on the development of the capacity/outage probability analyses. This study was supported in part by the State of Pernambuco Research Foundation (FACEPE) and the Brazilian Council for Scientific and Technological Development (CNPq).

Appendix A. The FFT-SP algorithm

Let Q_{it}^a the message sent from a variable node v_i to a check node f_t, while the message sent from a check node f_t to a variable node v_i is denoted by R_{ti}^a, where $a \in GF(q)$.

(1) **Initialization**: The algorithm is initialized from the calculation of the probability vector $\mathbf{p}_i = [p_i^0, \ldots, p_i^a, \ldots, p_i^{q-1}]$, where $p_i^a = p(v_i = a), a \in \{0, 1, \ldots, q-1\}$ is the probability of the ith transmitted symbol is equal to each one of the $GF(q)$ symbols (in ascending order), which is obtained by

$$p_i^a = \prod_{j=1}^{m} p(x_i^j | y_{d,i}^j) \tag{A.1}$$

in which $p(x_i^j | y_{d,i}^j)$ are the *a posteriori* probability of the antipodal signal x_i^j, with $x_i^j \in \{-1, +1\}$, representing the jth bit of the binary representation of the symbol $v_i = a$. The probabilities $p(x_i^j | y_{d,i}^j)$ are calculated according to:

$$p(x_i^j = +1 | y_{d,i}^j) = \frac{1}{1 + \exp(-4\Re(y_{d,i}^j))} \tag{A.2}$$

and $p(x_i^j = -1 | y_{d,i}^j) = 1 - p(x_i^j = +1 | y_{d,i}^j)$. Eq. (A.2) is obtained based on similar computations to those ones contained in [21]. Thus, the messages Q_{it}^a are initialized such that $Q_{it}^a = P_i^a$. After that, the q components of Q_{it}^a are cyclically exchanged, generating the messages $\widetilde{Q}_{it}^a$. More details about the permutation can be found in [17].

(2) **Updating of the check nodes messages:** To establish the exchanged check nodes messages $\widetilde{R}_{ti}^a$, initially the FFT is applied to the messages $\widetilde{Q}_{i't}^a$ and, then, the product of these FFTs is calculated. At last, the inverse FFT of the product of the previously mentioned quantities is computed, such that

$$\widetilde{R}_{ti}^a = F^{-1}\left(\prod_{i' \in V_{t|i}} F\left(\widetilde{Q}_{i't}^a\right) \right) \tag{A.3}$$

where $F(\cdot)$ and $F^{-1}(\cdot)$ are the FFT and inverse FFT operators, respectively, and $V_{t|i}$ is the variable node set connected to the parity check node f_t, excepting v_i.

To simplify the operations related to the FFT computing, we refer to the fact, shown in [22], that the FFT $F(\cdot)$ over $GF(q)$ is reduced to the fast Hadamard transform (FHT). In turn, FHT is obtained by the $q \times q$-dimensional Walsh–Hadamard matrix. The elementar Walsh–Hadamard matrix (in $GF(2)$) is given by [22]

$$W_2 = \frac{1}{\sqrt{2}} \begin{bmatrix} 1 & 1 \\ 1 & -1 \end{bmatrix}. \tag{A.4}$$

From the matrix W_2, it is possible to determine the generalization of the Walsh-Hadamard matrix for any field $GF(q)$, $q = 2^b$, defined recursively as [22]

$$W_{2b} = \frac{1}{\sqrt{b}} \begin{bmatrix} W_b & W_b \\ W_b & -W_b \end{bmatrix}, \tag{A.5}$$

with $b \in \{2, 4, 8, \ldots, q/2\}$. Considering that the inverse Walsh–Hadamard is itself [22], the messages

$\widetilde{R}^a_{ti}$ can be calculated as

$$\widetilde{R}^a_{ti} = W_{2b}\left(\prod_{i' \in V_{t|i}} W_{2b}\widetilde{Q}^a_{i't}\right). \quad (A.6)$$

Finally, a depermutation (inverse permutation) is applied to the messages $\widetilde{R}^a_{ti}$, resulting in the messages R^a_{ti} [17].

(3) **Updating of the variable node messages:** Given the parity check messages, the variable nodes recalculate their messages according to

$$Q^a_{it} = \lambda_{it} p^a_i \prod_{t' \in C_{i|t}} R^a_{t'i} \quad (A.7)$$

in which λ_{it} is a normalizing constant such that $\sum_{a=0}^{q-1} Q^a_{it} = 1$ and $C_{i|t}$ is the check node set connected to the node v_i, excepting f_t. The updating of the messages Q^a_{it} characterizes an iteration of the algorithm.

(4) **Finalization:** In this step, the algorithm computes the pseudo *a posteriori* probabilities Q^a_i given by

$$Q^a_i = \lambda_i p^a_i \prod_{t \in C_i} R^a_{ti} \quad (A.8)$$

where λ_i is a normalizing constant such that $\sum_{a=0}^{q-1} Q^a_i = 1$ and C_i is the check node set connected to the variable node v_i. After that, the decoder estimates which is the most probable value for each coded symbol, such that $\hat{v}_i = \arg\max_a Q^a_i$.

Given the estimate of the transmitted codeword ($\hat{\mathbf{v}}$), the decoding algorithm verifies if $\hat{\mathbf{v}}$ is a valid codeword. If it is not, the algorithm goes back to the Step 2, where the messages R^a_{ti} are computed again based on the messages Q^a_{it} (obtained in Step 3). The algorithm is ended only when $\hat{\mathbf{v}}$ is a valid codeword or when a maximum number of iterations is reached.

References

[1] J. Gubbi, R. Buyya, S. Marusic, M. Palaniswami, Internet of things (IoT): a vision, architectural elements, and future directions, Future Gener. Comput. Syst. 29 (7) (2013) 1645–1660, doi:10.1016/j.future.2013.01.010.

[2] M.S. Khan, M.S. Islam, H. Deng, Design of a reconfigurable RFID sensing tag as a generic sensing platform toward the future internet of things, IEEE Int. Things J. 1 (4) (2014) 300–310, doi:10.1109/JIOT.2014.2329189.

[3] S. Tozlu, Wi-fi enabled sensors for internet of things: a practical approach, IEEE Commun. Mag. 50 (6) (2012) 134–143, doi:10.1109/MCOM.2012.6211498.

[4] C.S. Bontu, S. Periyalwar, M. Pecen, Wireless wide-area networks for internet of things: an air interface protocol for IoT and a simultaneous access channel for uplink IoT communication, IEEE Veh. Technol. Mag. 9 (1) (2014) 54–63, doi:10.1109/MVT.2013.2295068.

[5] I.F. Akyildiz, T. Melodia, K.R. Chowdury, Wireless multimedia sensor networks: a survey, IEEE Wirel. Commun. Mag. 14 (6) (2007) 32–39, doi:10.1109/MWC.2007.4407225.

[6] K.J.R. Liu, A.K. Sadek, W. Su, A. Kwasinski, Cooperative Communications and Networking, Cambridge University Press, 2009.

[7] H. Fang, X. Lin, T. Lok, Power allocation for multiuser cooperative communication networks under relay-selection degree bounds, IEEE Trans. Veh. Technol. 61 (7) (2012) 2991–3001, doi:10.1109/TVT.2012.2200705.

[8] Y.W. Marye, H.A. Zhao, Optimum power allocation based adaptive modulation for cooperative wireless networks, in: Proceedings of the 2014 14th International Symposium on Communications and Information Technology (ISCIT 2014), 2014, pp. 323–326, doi:10.1109/ISCIT.2014.7011925.

[9] A. Chakrabarti, A.D. Baynast, A. Sabharwal, B. Aazhang, Low density parity check codes for the relay channel, IEEE J. Sel. Areas Commun. 25 (2) (2007) 280–291, doi:10.1109/JSAC.2007.070205.

[10] J. Cances, V. Meghdadi, Optimized low density parity check codes designs for half duplex relay channels, IEEE Trans. Wirel. Commun. 8 (7) (2009) 3390–3395, doi:10.1109/TWC.2009.080771.

[11] M.C. Davey, D.J.C. MacKay, Low density parity check codes over $GF(q)$, IEEE Commun. Lett. 2 (6) (1998) 165–167, doi:10.1109/ITW.1998.706440.

[12] IEEE 802.11n-2009 Wireless LAN Medium Access Control (MAC) and Physical Layer (PHY) Specifications: Enhancements for Higher Throughput, IEEE Std. 802.11, 2009.

[13] D.G. Brennan, Linear diversity combining technique, in: Proceedings of the IEEE, vol. 91, 2003, pp. 331–356, doi:10.1109/JPROC.2002.808163.

[14] L. Conde-Canencia, A. Al-Ghouwayel, E. Boutillon, Complexity comparison of non-binary LDPC decoders, in: Proceedings of ICT Mobile Summit, 2009, pp. 1–8. ISBN:978-1-905824-12-0.

[15] D.J.C. Mackay, M.C. Davey, Evaluation of Gallager codes for short block length and high rate applications, Codes, Syst. Graph. Models 123 (1999) 113–130.

[16] F.R. Kschischang, B.J. Frey, H.A. Loeliger, Factor graphs and the sum-product algorithm, IEEE Trans. Inf. Theory 47 (2) (2001) 498–519, doi:10.1109/18.910572.

[17] R.A. Carrasco, M. Johnston, Non-Binary Error Control Coding for Wireless Communication and Data Storage, John Wiley & Sons Ltd., 2008.

[18] J.N. Laneman, D.C. Tse, G. Wornell, Cooperative diversity in wireless networks: Efficient protocols and outage behavior, IEEE Trans. Inf. Theory 50 (12) (2004) 3062–3080, doi:10.1109/TIT.2004.838089.

[19] A. Goldsmith, Wireless Communication., Cambridge University Press, 2005.

[20] R. Knopp, P. Humblet, On coding for block fading channels, IEEE Trans. Inf. Theory 46 (1) (2000) 189–205, doi:10.1109/18.817517.

[21] H.V. Khuong, H.Y. Kong, Performance analysis of cooperative communications protocol using sum-product algorithm for wireless relay networks, in: Proceedings of the IEEE 8th International Conference on Advanced Communications Technology (ICACT 2006), 2006, pp. 2168–2173, doi:10.1109/ICACT.2006.206429.

[22] X. Li, M.R. Soleymani, A proof of the Hadamard transform decoding of the belief propagation algorithm for LDPCC over $GF(q)$, in: Proceedings of the IEEE 60th Vehicular Technology Conference (VTC 2004-Fall), 2004, pp. 2518–2519, doi:10.1109/VETECF.2004.1400507.

Bruna L. R. Melo received the B.Sc. degree in electrical engineering with emphasis on telecommunications (2010) and received the M.Sc. degree in systems engineering (2013), both from University of Pernambuco in Recife-PE, Brazil. She currently works as air traffic controller for Brazilian Air Force at Recife-PE, Brazil. Her current research interests are focused on cooperative communications, satellite communications and machine learning techniques.

Daniel C. Cunha received the M.Sc. and Ph.D. degrees in electrical engineering from the State University of Campinas (UNICAMP), in 2003 and 2006, respectively. He is currently an adjunct professor of Computer Science and Computer Engineering at the Centro de Informtica of the Federal University of Pernambuco (CIn/UFPE), Recife-PE, Brazil. Formerly, he was an adjunct professor of Telecommunications Engineering at University of Pernambuco (UPE), Recife-PE, from 2007 to 2012. His contributions are in the area of error control coding, cooperative communications and machine learning techniques applied to telecommunications systems. His current research interests are in mobile positioning systems and power consumption of mobile devices.

Cecilio Pimentel was born in Recife, Brazil, in 1966. He received the B.Sc. degree from the Federal University of Pernambuco, Recife, Brazil, in 1987; the M.Sc. degree from the Catholics University of Rio de Janeiro, Rio de Janeiro, Brazil, in 1990; and the Ph.D. degree from the University of Waterloo, Ontario, Canada, in 1996, all in electrical engineering. Since October 1996, he has been with the Department of Electronics and Systems at the Federal University of Pernambuco, where he is currently an Associate Professor. From 2007 to 2008, he was a Visiting Research Scholar at the Department of Mathematics and Statistics, Queen's University, Kingston, Canada. His research interests include digital communications, information theory, and error correcting coding.